Dyes and Pigments 254 (2026) 113902

Contents lists available at ScienceDirect

Dyes and Pigments

journal homepage: www.elsevier.com/locate/dyepig

A new ultra-fast and sensitive chemosensor based on NIR chromenylium-cyanine molecule modified with thiazole unit for the detection of Hg^{2+} in real samples

Utku Ertugral [a], Hulya Aribuga [a], Ozgur Yavuz [a], Emre Ozdemir [a], Yusuf Alcay [a], Nebahat Ejder [b], Ismail Yilmaz [a,*]

[a] Istanbul Technical University, Department of Chemistry, Maslak, Istanbul, 34469, Turkey
[b] Recep Tayyip Erdogan University, Faculty of Medicine, Department of Medical Microbiology, Rize, Turkey

ARTICLE INFO

Keywords:
Mercury
Chromenylium cyanine
Smartphone
Fluorescence
Near-infrared

ABSTRACT

Since Hg^{2+} ion contamination constitutes a global threat, the necessity for a rapid, selective and sensitive sensing methods for Hg^{2+} ions has attracted growing research interest in recent years. Herein, we present the development of a new "ratiometric" and "turn-on" fluorescent probe **NIR-12** having absorption and emission properties within the near-infrared (NIR) spectrum. The probe was constructed on a chromenylium cyanine platform decorated with 2-amino-5-bromothiazole for the purpose of efficiently detecting Hg^{2+} ions in an aqueous medium. Structural analysis of **NIR-12** and its interaction with Hg^{2+} ions were confirmed by several spectrophotometric techniques. The non-fluorescent probe **NIR-12** selectively interacted with Hg^{2+} ions, resulting in a ring opening on the platform. This process led to the generation of strong NIR absorption and emission signals, as well as a substantial color change. Consequently, this enabled the execution of colorimetric analyses. The probe responded to Hg^{2+} ions very rapidly within 10 s, and exhibited wide linear ranges (1.68-9.81 μM for UV-Vis and 0.85-42.98 μM for fluorescence methods) and remarkably low detection limits for Hg^{2+} ions (LOD) (0.057 μM (11.40 ppb) for UV-Vis, 0.277 μM (55.53 ppb) for fluorescence). The probe was also applied to real drinking water samples with high recovery ranges (95.13% - 106.62%). The application of smartphone-assisted analysis for Hg^{2+} ions was thoroughly investigated, demonstrating a linear range between 5.32×10^{-8} M and 9.49×10^{-6} M and a low LOD of 3.42×10^{-6} M.

1. Introduction

Engineering innovative molecular probes for the detection and real-time tracking of toxic metal ions, particularly within biological and environmental contexts, has recently become a highly significant research focus [1–6]. Mercury (Hg^{2+}) has been found in a variety of everyday products. These include batteries, thermometers, jewelry, paints, pesticides, barometers, dental amalgams, and electronic devices. Despite its ubiquity, it is regarded as one of the most hazardous and persistent environmental pollutants [7–10]. Mercury, present in ionic, metallic, inorganic, and organic forms, is recognized as highly toxic even at trace levels. Its occurrence in water systems constitutes a serious environmental and public health issue. After entering the body, mercury can interfere with neurological and endocrine functions, producing long-lasting systemic damage and posing particular risks during fetal development [11–13]. According to the U.S. Environmental Protection Agency (EPA), the maximum concentration of inorganic mercury in drinking water is 2 ppb, emphasizing the high toxicity of mercury [14, 15].

A variety of analytical techniques are currently employed for the determination of Hg^{2+} ions, for instance, inductively coupled plasma-atomic emission spectrometry (ICP-AES) [16], atomic absorption spectroscopy (AAS) [17], voltammetric methods [18], infrared spectroscopy (IR) [19], and atomic fluorescence spectrometry (AFS) [20]. Even though these conventional analytical techniques are effective and provide both precise and sensitive results, they are limited by high instrumentation costs, time-consuming sample preparation, and the need for skilled operators. To address these limitations, targeted fluorogenic and colorimetric chemosensors have recently attracted considerable attention from researchers due to their ease of use in biological and

* Corresponding author.
E-mail address: iyilmaz@itu.edu.tr (I. Yilmaz).

https://doi.org/10.1016/j.dyepig.2026.113902
Received 3 March 2026; Received in revised form 22 May 2026; Accepted 26 May 2026
Available online 27 May 2026

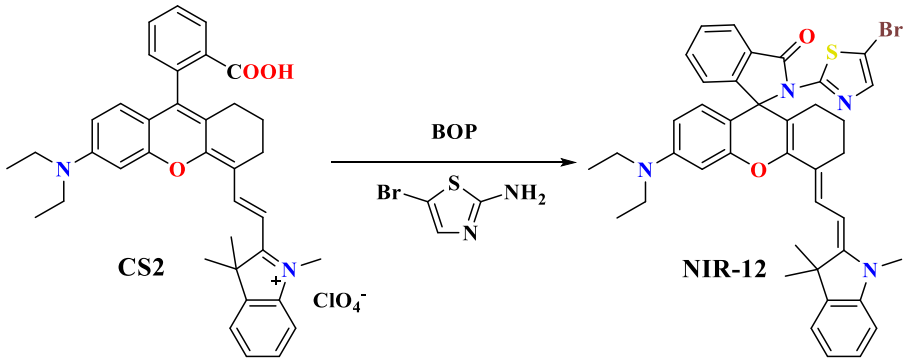

Fig. 1. Synthesis route for probe **NIR-12**.

environmental samples, capability for visual detection, and high selectivity and sensitivity [21–26].

Numerous organic fluorometric and colorimetric compounds, such as rhodamine [27], pyrene [28], BODIPY [29], coumarin [30], quinoline [31], and cyanine [32], have been documented across literature as effective approaches for identifying Hg^{2+} ions. Despite their usefulness, many of these platforms exhibit weak stability in complex matrices, long response times, and, most importantly, emission wavelengths below 650 nm, restricting their applicability in biological studies.

Near-infrared (NIR) organic platforms with emission wavelengths above 650 nm have become increasingly popular, especially for chemosensor development and biological applications, owing to strong tissue penetration, low tissue damage, and minimal background autofluorescence. In addition, NIR probes with high brightness and quantum efficiency are anticipated to provide enhanced sensitivity for detecting analytes [33–36].

The chromenylium-cyanine (CS) platform operates through a sensing mechanism closely resembling that of rhodamine and possesses a closed spirolactam ring after proper modification with convenient amines, resulting in pale-yellow, "turn-off" fluorescence [37]. When exposed to a suitable analyte or acidic conditions, the ring opens, extending conjugation throughout the molecule. Consequently, this results in the generation of a strong absorbance and fluorescence responses within the NIR spectral range (>700 nm), and promoting a visible color change to green. The open-ring structures generally exhibit high quantum yields, making CS platforms highly suitable for both chemosensing and biological imaging applications [21,22,24,38].

In light of these hypotheses, the CS-based rigid **NIR-12** chemosensor decorated with 2-amino-5-bromothiazole was designed and synthesized for the first time. In its closed spirolactam form, **NIR-12** remains in a fluorescence "off" state. When Hg^{2+} ions are introduced, hydrolysis induces a ring opening which gives rise to the formation of the CS2 molecule (the acid form), and the resulting extended conjugation leads to strong absorption at 717 nm and intense emission at 740 nm. Probe **NIR-12** showed great limits of detection (LOD) (0.057 μM (11.40 ppb) for UV-Vis, 0.277 μM (55.53 ppb) for fluorescence) with a wide linear range (1.68-9.81 μM for UV-Vis and 0.85-42.98 μM for fluorescence methods), ultrafast response time of 10 s, and excellent selectivity and sensitivity for Hg^{2+} ions detection. Moreover, the probe **NIR-12** demonstrated high recovery ranges (95.13% - 106.62%) for real drinking water sample analysis. In addition, the sharp color transition of the probe in response to Hg^{2+} concentration allows sensitive on-site analysis, which can be readily performed by the naked eye, and with a smartphone, eliminating the need for complex equipment. In view of all these properties of **NIR-12**, the comparison table clearly demonstrates that the probe outperforms many previously reported probes. Also, the following section outlines five important examples of probes designed to sense Hg^{2+} ions. Du et al. developed probe InRhH which is an indazole-fused rhodamine fluorescent probe, for the selective and sensitive detection of Hg^{2+} ions [39]. The probe detects via a fluorescence "off-on" mechanism, accompanied by an observable shift in color, which is initiated by the Hg^{2+} induced spirolactam ring opening in an aqueous acetonitrile medium (CH_3CN/H_2O, v/v, pH 6.0). This sensing system demonstrated a low LOD (0.33 nM) and a response time of 40 min. Furthermore, the practical applicability of InRhH was successfully established through fluorescence imaging experiments in living HeLa cells and tracing using test strips. Hong et al. reported a rhodamine-based fluorescent probe (RTTU) for detection of Hg^{2+} ions in acetonitrile/HEPES medium (9/1, v/v, pH 7.21) [40]. The probe exhibits a linear fluorescence response between 25 μM and 200 μM, a detection limit of 3.04×10^{-7} M, and the maximum signal was achieved within 30 min. Also, the probe demonstrated selectivity and applicability for Hg^{2+} ions in real water samples. Liu and Qian designed a chemodosimeter (REPN), composed of 1,8-naphthalimide and rhodamine units, as a ratiometric fluorescent sensor for Hg^{2+} and Fe^{3+} detection [41]. The reported detection limit for Hg^{2+} was 2.72×10^{-6} M. The probe demonstrates a markedly lower sensitivity toward Hg^{2+} compared to Fe^{3+} (LOD = 5.7×10^{-7} M). Zhang et al. synthesized a rhodamine-anthracene based ratiometric fluorescent probe. The probe exhibited high specificity for Hg^{2+} ions and worked with FRET mechanism [42]. The detection limit for Hg^{2+} ions was reported as 0.38 μM. Additionally, the probe was demonstrated to be applicable for Hg^{2+} imaging in living cells. Biswal et al. synthesized two rhodamine based probes coupled with substituted pyrroles (Probe 1 and Probe 2) [43]. Both probes showed interaction for Hg^{2+}, Fe^{2+} and Pb^{2+} ions. The response time for Probe 1 to Hg^{2+} was determined as 15 min. Limit of detection was calculated as 0.6 nM. Also, imaging Hg^{2+} ions in living E. coli cells were successfully tested. Considering all these parameters (response time, selectivity, applicability to real samples, etc.) there remain unmet needs in the literature regarding chemosensors for the detection of Hg^{2+} ions. Therefore, owing to its low limit of detection, rapid response and high selectivity the probe (**NIR-12**) developed in this study is anticipated to make a noteworthy contribution to the literature of sensor studies.

2. Experimental section

2.1. Materials and instruments

Supplementary Materials have been provided for further information regarding the chemicals and instrumentation utilized in this study.

2.2. Synthesis of NIR-12

Fig. 1 represents the synthesis of **NIR-12** probe starting from CS2 compound which was synthesized according to the literature [44]. The synthetic route and characterization of CS2 compound were shared in Supporting Information (Figure S1-S7). CS2 (0.66 g, 1 mmol) and

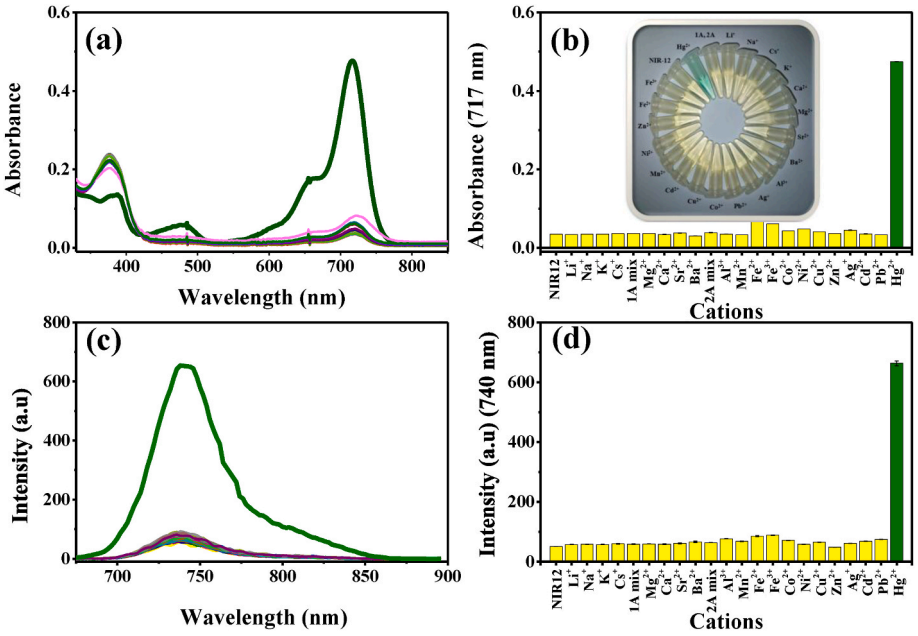

Fig. 2. (a) UV-Vis and (c) fluorescence spectra of the probe **NIR-12** (1×10^{-5} M) in the presence of various cations (5×10^{-5} M), and the corresponding (b) absorbance (b,inset) colorimetric responses for several analytes, and (d) emission intensity bar graphs in EtOH/H_2O (3/1, v/v, pH 7.4 HEPES). (λ_{ex} = 650 nm, slit width = 5 nm × 10 nm).

benzotriazole-1-yl-oxy-tris-(dimethylamino)-phosphoniumhexafluoro phosphate (BOP) reagent (0.44 g, 1 mmol) were mixed in dry dichloromethane (DCM) (15 mL) under N_2 atmosphere for 30 min. Then, 2-amino-5-bromothiazole monohydrobromide (0.52 g, 2 mmol) is dissolved in triethylamine (1 mL) and it is gradually added into the mixture while under continuous stirring in an ice bath. Following the completion of the addition step, stirring was maintained for 2 h at room temperature [45]. Then, the solvent of the mixture was then removed under reduced pressure. The obtained residue was dissolved in DCM, followed by sequentially washing with brine and water. Afterwards, the organic layer was isolated and dried with Na_2SO_4. After that, the product was purified via silica gel column chromatography employing ethyl acetate/hexane (1/10, v/v) as the mobile phase. As a result, a pure **NIR-12** probe is obtained as yellow powder (yield 61%). ^{1}H NMR (Figure S8) (500 MHz, DMSO-d_6) δ 7.95 (d, J = 7.7 Hz, 1H), 7.71 (td, J = 7.5, 1.2 Hz, 1H), 7.61 (t, J = 7.5 Hz, 1H), 7.50 (s, 1H), 7.41 (d, J = 12.6 Hz, 1H), 7.31 – 7.26 (m, 1H), 7.14 (td, J = 7.7, 1.3 Hz, 1H), 6.86 – 6.75 (m, 2H), 6.32 – 6.21 (m, 3H), 5.38 (d, J = 12.7 Hz, 1H), 3.29 (t, J = 7.0 Hz, 3H), 3.13 (s, 3H), 2.47 – 2.17 (m, 2H), 1.65 (d, J = 14.5 Hz, 6H), 1.58 – 1.46 (m, 1H), 1.45 – 1.27 (m, 4H), 1.24 (d, J = 12.7 Hz, 1H), 1.07 (t, J = 7.0 Hz, 6H). ^{13}C NMR (Figure S9) (126 MHz, DMSO-d_6) δ 166.91, 157.74, 155.35, 152.24, 152.18, 148.67, 146.97, 145.43, 139.79, 138.63, 135.63, 129.80, 128.19, 127.64, 127.17, 124.20, 123.81, 122.08, 119.85, 119.78, 119.71, 108.37, 106.61, 105.55, 103.48, 103.32, 97.39, 92.45, 69.83, 45.37, 44.02, 29.36, 28.57, 25.11, 22.96, 22.04, 12.85. APT, COSY, HSQC and HMBC NMR studies were performed as other characterization methods and are shared in Figures S10-S13. HRMS m/z: observed peak at 721.20343 corresponding to the $[M+H]^+$ peak consist of isotopic Br ion (^{81}Br) calculated accordingly for $C_{40}H_{39}BrN_4O_2S$ $[M]^+$: 720.19566 (Figure S14). FT-IR (ATR) (cm^{-1}): 3055 (=C–H), 2973 (-C-H), 1703 (C═O), 1617 (C═N) (Figure S15).

2.3. Solutions and optical studies

The stock solution of the **NIR-12** probe was generated using ethanol (1×10^{-4} M) as the solvent. The stock solution of the analytes (Li^+, Na^+, Cs^+, K^+, Ca^{2+}, Mg^{2+}, Sr^{2+}, Ba^{2+}, Al^{3+}, Ag^+, Pb^{2+}, Co^{2+}, Cu^{2+}, Cd^{2+}, Mn^{2+}, Ni^{2+}, Zn^{2+}, Fe^{2+}, Fe^{3+} and Hg^{2+}) (5×10^{-2} M) as perchlorate salts were prepared using deionized water. The sensor studies were conducted with the solution of the probe **NIR-12** (1×10^{-5} M) prepared in EtOH/H_2O (3/1, v/v, pH 7.4 HEPES (1 mM)) according to optimization studies shown in Figure S16. All experiments were conducted in triplicate at room temperature. An excitation wavelength of 650 nm was utilized, and the slit widths for excitation and emission were adjusted to 5 and 10 nm, in that sequence. During the titration experiments, the concentration of probe **NIR-12** was maintained at 1×10^{-5} M to ensure optimal analytical performance.

2.4. Preparation of solutions for use in the smartphone-based analysis

The capability of probe **NIR-12** for smartphone based Hg^{2+} detection was thoroughly examined using a Samsung S24 FE smartphone. For this study, the quartz cuvette was placed securely in a holder inside a small studio and filled with the probe **NIR-12** in EtOH/H_2O (3/1, v/v, pH 7.4 HEPES). Subsequently, a titration study with Hg^{2+} ions was performed, and every image was captured after each addition of Hg^{2+} ions. The collected data were processed to obtain RGB values. The Green values versus Hg^{2+} concentration exhibited the best linear correlation for the smartphone titration study.

2.5. Measurements of Hg^{2+} concentrations in different real samples

The probe **NIR-12** was tested to detect Hg^{2+} ions in real sample matrices. Therefore, three commercial drinking water brands were acquired. Each real sample was diluted tenfold using ultrapure water. Then, various concentrations within the determined linear range were carefully selected and analyzed using both UV-Vis and fluorescence spectroscopic methods.

3. Results and discussion

3.1. Design and synthesis

Here, a 2-amino-5-bromothiazole-appended CS rigid platform (**NIR-12**) was designed and utilized for the selective and sensitive detection of Hg^{2+} ions. In its ring-closed form, **NIR-12** exhibits no fluorescence and

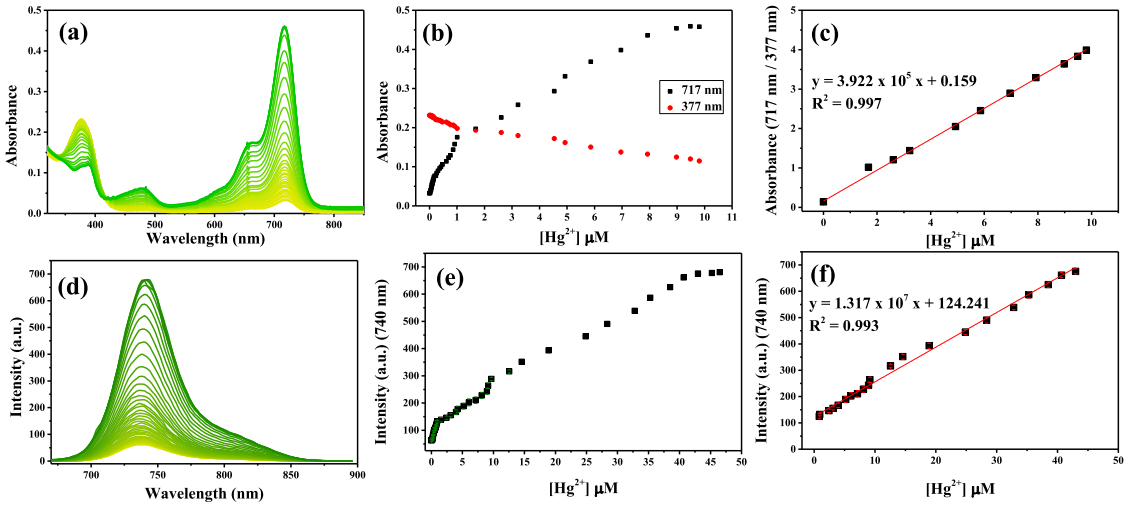

Fig. 3. Titration study of probe **NIR-12** (1×10^{-5} M) for Hg^{2+} ions in EtOH/H_2O (3/1, v/v, pH 7.4 HEPES). For UV-Vis method (a) spectral changes, (b) ratiometric response, (c) linear range. For fluorescence method (d) spectral changes, (e) total signals of titration study (f) linear range. (λ_{ex} = 650 nm, slit width = 5 nm × 10 nm).

displays a pale-yellow color. Upon the addition of Hg^{2+}, a process of hydrolysis induces a ring opening, thereby generating the CS2 acid form. This results in strong absorption (717 nm) and emission (740 nm) in the NIR region, enhanced quantum yield, and an observable color shift from pale yellow to bright green. This platform represents a new generation of molecular design in sensor chemistry. The incorporation of the 2-amino-5-bromothiazole moiety imparts selective recognition of Hg^{2+}, attributed to the high affinity of the thiazole sulfur towards Hg^{2+} ions, as well documented in the literature [45–47].

Synthesis of **NIR-12** was accomplished through the nucleophilic addition of 2-amino-5-bromothiazole to the CS2 intermediate in the presence of BOP reagent, which promotes the amidification reaction. The CS2 precursor was synthesized following reported procedures [44]. Subsequent purification of **NIR-12** by column chromatography afforded the pure pale-yellow product in high yield (61%). The characterization of the probe **NIR-12** is presented in Figures S8-S15. Solvent/water ratio and response time optimization for sensor studies were investigated and shared in Figures S16–18. Furthermore, **NIR-12** and its molecular interaction with Hg^{2+} ion (Figure S19 and 20) were thoroughly investigated using nuclear magnetic resonance (^{1}H NMR, ^{13}C NMR, APT, HMBC, HSQC NMR), Fourier-transform infrared spectroscopy (FT-IR), high-resolution mass spectrometry (HR-MS), UV-Vis, and fluorescence spectroscopic techniques.

3.2. Spectrophotometric properties and optimization

To investigate spectrophotometric properties, the UV-Vis absorbance and fluorescence emission spectra of the **NIR-12** probe in varying concentrations of ethanol solution were recorded (Figure S16). The obtained spectra showed that the probe had no absorption or emission in the visible region (400-750 nm). To determine the solvent conditions in which spectrophotometric studies would be conducted, Hg^{2+} ion was added to the probe in EtOH/H_2O mixtures at different ratios, and then the UV-Vis and fluorescence responses were recorded. Upon introduction of Hg^{2+} ions, a new absorption band at 719 nm appeared in the UV-Vis spectrum and a new emission intensity at 745 nm in the fluorescence spectrum. As a result of tests conducted in varying EtOH/H_2O mixtures, the most ideal signals were obtained in EtOH/H_2O (3/1, v/v) (Figure S16). The pH-dependent optical behavior of **NIR-12**, both in the absence and presence of Hg^{2+} ions was carefully studied and recorded by UV-Vis and fluorescence methods (Figure S17). Consequently, EtOH/H_2O (3/1, v/v, pH 7.4 HEPES) medium was selected as the operating condition, and all spectrophotometric studies were conducted in this environment.

To evaluate the response time for sensor studies, the response of the **NIR-12** probe to Hg^{2+} ion was recorded over time. It was observed that the UV-Vis and fluorescence signals of the **NIR-12** probe increased immediately after the addition of Hg^{2+} ion, and within 10 s this increase remained constant (Figure S18). Therefore, the response time was established as 10 s, and this response time was used in all spectrophotometric studies. The ability of **NIR-12** to detect Hg^{2+} ions so quickly is a prominent feature for real-time detection. A very rapid response is especially critical for the practical application of chemosensors, allowing on-site and fast analysis in environmental matrices [48].

3.3. Selectivity study

To investigate the spectral response of **NIR-12** for various cations, Li^+, Na^+, Cs^+, K^+, Ca^{2+}, Mg^{2+}, Sr^{2+}, Ba^{2+}, Al^{3+}, Ag^+, Pb^{2+}, Co^{2+}, Cu^{2+}, Cd^{2+}, Mn^{2+}, Ni^{2+}, Zn^{2+}, Fe^{2+}, Fe^{3+}, Hg^{2+}, 1A group mixture and 2A group mixture (5×10^{-5} M) were individually added to a solution of probe **NIR-12** (1×10^{-5} M) prepared in EtOH/H_2O (3/1, v/v, pH 7.4 HEPES), and UV-Vis and fluorescence spectra were recorded. As presented in Fig. 2, a significant spectral change was recognized solely upon the introduction of Hg^{2+} ions. The presence of Hg^{2+} ions caused an increase in absorbance at 717 nm in the UV-Vis and emission signal at 740 nm in the fluorescence spectrum (Fig. 2a and c). This selective enhancement of the spectral response shows that probe **NIR-12** exhibits high specificity toward Hg^{2+} ions among all studied cations. Fig. 2b and d shows bar graphs of the absorbance signal at 717 nm and emission intensity at 740 nm of probe **NIR-12**, respectively. As shown these graphs, the spectral changes caused by the Hg^{2+} ion were very significant compared to other cations.

3.4. Titration study and LOD

The spectral responses of probe **NIR-12** in EtOH/H_2O (3/1, v/v, pH 7.4 HEPES) increased proportionally with the gradual addition of Hg^{2+} ions. As shown in Fig. 3a–b, while the absorbance signal at 717 nm was enhanced, the band at 377 nm was declined with the addition of Hg^{2+} ions, which indicates a ratiometric response in UV-Vis spectrum. This ratiometric behavior provides superior analytical accuracy of the method when compared to relying single absorption signal. As illustrated in Fig. 3d, the fluorescence intensity at 740 nm increased with the

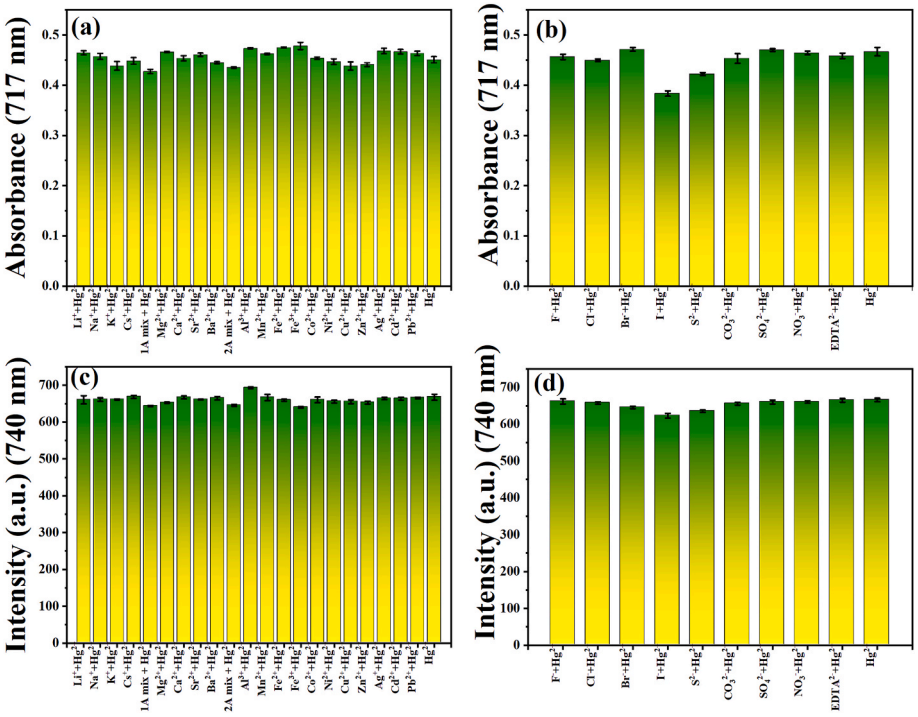

Fig. 4. UV-Vis responses of the probe **NIR-12** (1×10^{-5} M) in the presence of various cations (5×10^{-5} M) (a) and anions (5×10^{-5} M) (b), and the fluorescence emission responses in the presence of various cations (5×10^{-5} M) (c) and anions (5×10^{-5} M) (d) of probe **NIR-12** (1×10^{-5} M) EtOH/H_2O (3/1, v/v, pH 7.4 HEPES). (λ_{ex} = 650 nm, slit width = 5 nm × 10 nm).

addition of Hg^{2+} ions. The linear ranges of these signals were shown in Fig. 3c–f. Accordingly, Hg^{2+} concentrations with the range of 1.68 - 9.81 μM and 0.85 - 42.98 μM were found to be working linear ranges for probe **NIR-12** for the UV-Vis and fluorescence methods, respectively. Moreover, LOD values of probe **NIR-12** for Hg^{2+} ions were calculated using the 3×σ/k equation in the light of titration experiments. The LOD values were calculated as 0.057 μM (11.40 ppb) for the UV-Vis method and 0.277 μM (55.53 ppb) for the fluorescence method. These LOD values shows that probe **NIR-12** exhibits superior sensitivity for Hg^{2+} ion detection compared with similar probes reported in the literature.

3.5. Examination of interference effects

Interference experiments were carried out to examine the detection ability of probe **NIR-12** toward Hg^{2+} ions in a medium containing a range of other cations and anions. For this purpose, individual solutions of Li^+, Na^+, Cs^+, K^+, Ca^{2+}, Mg^{2+}, Sr^{2+}, Ba^{2+}, Al^{3+}, Ag^+, Pb^{2+}, Co^{2+}, Cu^{2+}, Cd^{2+}, Mn^{2+}, Ni^{2+}, Zn^{2+}, Fe^{2+}, Fe^{3+} cations (5×10^{-5} M) and F^-, Cl^-, Br^-, I^-, S^{2-}, CO_3^{2-}, SO_4^{2-}, NO_3^-, $EDTA^{2-}$ anions (5×10^{-5} M) were added to **NIR-12** (1×10^{-5} M) in EtOH/H_2O (3/1, v/v, pH 7.4 HEPES) medium. Then, Hg^{2+} ion (5×10^{-5} M) was introduced separately into each solution, and the corresponding UV-Vis and fluorescence spectra were recorded. As depicted in Fig. 4, the absorbance and emission intensities of **NIR-12** probe in the coexistence of Hg^{2+} ion were not affected by the presence of other cations or anions. Hence, these results clearly exhibit the effective selectivity and strong resistance to interference of **NIR-12** for sensing Hg^{2+} ions in water.

3.6. Proposed binding mechanism between NIR-12 and Hg^{2+}

The proposed sensing mechanism proceeds via the Hg^{2+}-induced hydrolysis of **NIR-12** generating the corresponding acid derivative, CS2, which triggers a transition from a fluorescence "off" state to an activated "on" state. To prove the formation of CS2 compound, purification and characterization process were conducted after the addition of Hg^{2+} ions to NIR-12 solution. The purification was completed via column chromatography with silica gel as stationary phase and DCM/MeOH (15/1, v/v) as eluent system. The HR-MS spectra (Figure S19) confirms that the obtained mass of the product (**NIR-12**+Hg^{2+}) (m/z = 559.29401) is in excellent coherence with the calculated mass of CS2 derivative (m/z = 559.29552). Considering the ^{1}H NMR analysis (Fig. 5), the aromatic resonances of product (**NIR-12**+Hg^{2+}) exhibit noticeably downfield shifts relative to those of **NIR-12**, indicating that the spirolactam ring opens upon reaction with Hg^{2+}, reflecting the characteristic green color of the product CS2. In particular, the disappearance of alkenyl proton signal of **NIR-12** at 5.43 ppm and the appearance of a new signal associated with the acidic proton of the product (8.44) strongly support the formation of the acidic structure CS2. To further verify the proposed sensing mechanism, product (**NIR-12**+Hg^{2+}) spectrum was compared with CS2. The perfect alignment of the characteristic proton peaks provides strong support for the proposed reaction mechanism. In the FT-IR analysis (Figure S20), the structures **NIR-12**, the reaction product (**NIR-12**+Hg^{2+}), and CS2 were compared. As clearly seen, **NIR-12** exhibits no acidic –OH stretching band vibration around 3300 cm^{-1}, whereas the reaction product displays a strong –OH band, closely resembling that of CS2. Furthermore, the remaining characteristic bands of the product align well with those of CS2. Taken together with the HR-MS, NMR, and FT-IR results, these observations clearly demonstrate that the closed-ring spirolactam framework of **NIR-12** undergoes Hg^{2+} induced ring opening, yielding the acid derivative CS2.

3.7. Colorimetric analysis

The capability to detection via a simple color change, without requiring any additional instrumental equipment, represents a major advantage in sensor field. In this context, the colorimetric response of probe **NIR-12** toward Hg^{2+} ions provide an excellent feature for instantaneous, on-site analysis. As shown in Fig. 2b, the solution of **NIR-12** (1×10^{-5} M) on its own and in the presence of all cations (5×10^{-5} M) exhibited a pale yellow color in EtOH/H_2O (3/1, v/v, pH 7.4 HEPES),

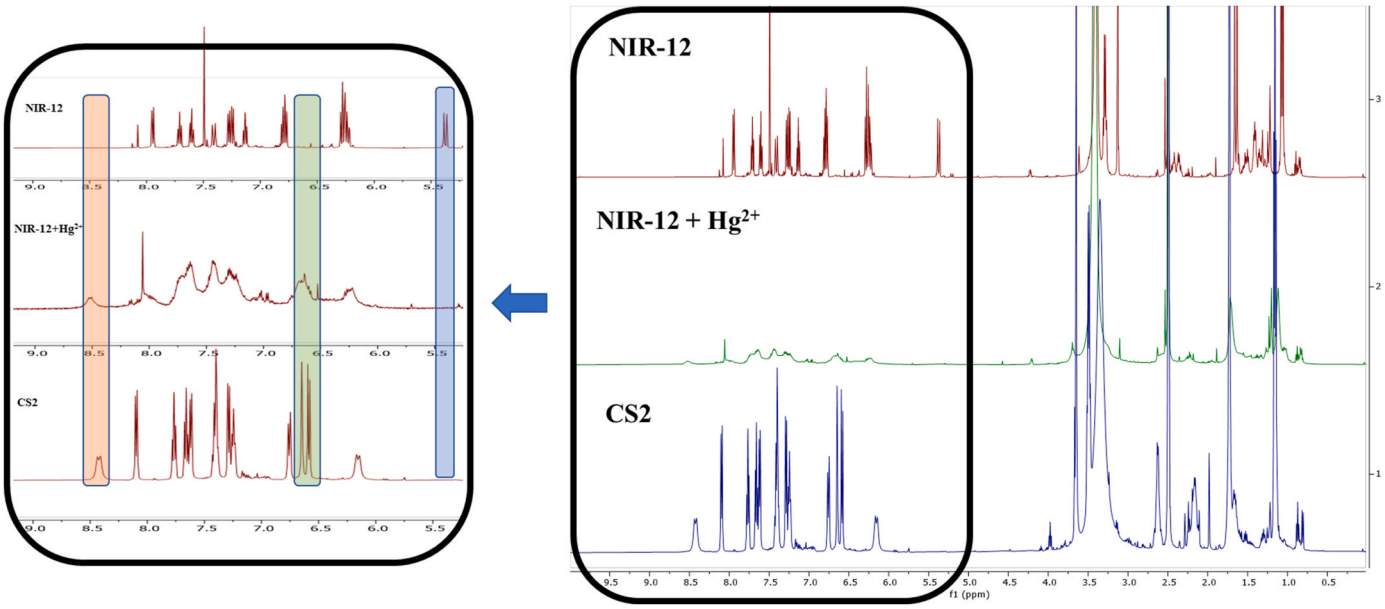

Fig. 5. Full ^{1}H NMR spectra of free **NIR-12**, **NIR-12**+**Hg^{2+}** and CS2 form together with the corresponding zoomed in region (5.0-9.0 ppm) which emphasize characteristic spectral signals.

whereas it turned green exclusively following the introduction of Hg^{2+} ions. The addition of other cations did not induce any remarkable color change, indicating that the colorimetric response of probe **NIR-12** is highly selective for Hg^{2+} ions in naked-eye detection.

3.8. Analysis of Hg^{2+} ions in real sample matrices

To investigate the capability of probe **NIR-12** to recognize Hg^{2+} in real sample environments, analyses were conducted using commercially available drinking water. Drinking water from three different brands was purchased from a local supermarket and added to the probe **NIR-12** in EtOH/H_2O (3/1, v/v, pH 7.4 HEPES). No remarkable changes were observed in the absorbance and fluorescence signals, indicating the exclusion of Hg^{2+} in untreated samples (as "Not Detected (ND)" in Table 1). Afterwards, known amounts of Hg^{2+} ions were introduced to the drinking water samples, and analyzed by using probe **NIR-12**. The concentrations found from these analyses were compared with the added concentrations to calculate recovery rates, which were shared in Table 1. The probe **NIR-12** exhibited excellent analytical performance, achieving recovery rates between 95.13% and 106.62%, confirming its suitability for the quantification of Hg^{2+} ions in real water samples.

3.9. Determination of Hg^{2+} using smartphone-based analysis

The Hg^{2+} levels in a given sample can be quantified by monitoring the color shift of the **NIR-12** solution by using a smartphone camera. The fluorescent cuvette was placed in a photography studio with a fixed position. Then, the EtOH/H_2O (3/1, v/v, pH 7.4 HEPES) solution of the **NIR-12** (1×10^{-5} M) probe was placed in this cuvette, and the solution was gradually treated with Hg^{2+} ions (Figure S21). After each addition, the images were captured with a smartphone camera (Samsung Galaxy S24 FE). Three different points were selected from these photographs to determine the RGB (Red-Green-Blue) values. A linear calibration plot was constructed, with an R^2 value of 0.991, by graphing various combinations of RGB values against the Hg^{2+} ion concentrations. The calibration curve was plotted using the Green values on the y-axis, and the corresponding equation of the plot was expressed as $y = -505836.423x + 165.882$. The obtained linear range was found between 5.32×10^{-8} M to 9.49×10^{-6} M Hg^{2+} ion concentrations, and LOD value was calculated as 3.42×10^{-6} M. Fig. 6 shows visible-light photographs of the

Table 1
Recovery and RSD values of probe **NIR-12** for three different commercial drinking water samples for Hg^{2+} quantification by using a) UV-Vis and b) fluorescence method.

a)	Drinking Water 1			Drinking Water 2			Drinking Water 3		
Added (mg/L)	Found (mg/L)	Recovery (%)	RSD (±)	Found (mg/L)	Recovery (%)	RSD (±)	Found (mg/L)	Recovery (%)	RSD (±)
0	ND	-	-	ND	-	-	ND	-	-
0.34	0.35	103.38	0.01	0.36	106.62	0.02	0.33	97.73	0.01
0.65	0.63	96.82	0.02	0.63	96.95	0.01	0.62	96.05	0.02
1.18	1.17	99.48	0.01	1.16	98.66	0.01	1.15	97.37	0.02
1.59	1.66	104.63	0.05	1.62	101.84	0.02	1.64	103.24	0.04
1.90	1.96	103.25	0.04	1.93	101.63	0.02	1.94	101.95	0.03
b)	**Drinking Water 1**			**Drinking Water 2**			**Drinking Water 3**		
Added (mg/L)	**Found (mg/L)**	**Recovery (%)**	**RSD (±)**	**Found (mg/L)**	**Recovery (%)**	**RSD (±)**	**Found (mg/L)**	**Recovery (%)**	**RSD (±)**
0	**ND**	**-**	**-**	**ND**	**-**	**-**	**ND**	**-**	**-**
0.19	0.18	97.60	0.01	0.19	97.77	0.01	0.18	95.13	0.01
0.62	0.61	98.75	0.01	0.61	97.81	0.01	0.63	101.22	0.01
1.04	1.06	102.06	0.02	1.04	99.51	0.01	1.04	100.06	0.01
1.43	1.45	101.59	0.02	1.47	102.96	0.03	1.49	104.23	0.04
1.83	1.83	99.26	0.01	1.82	98.96	0.01	1.81	98.59	0.02

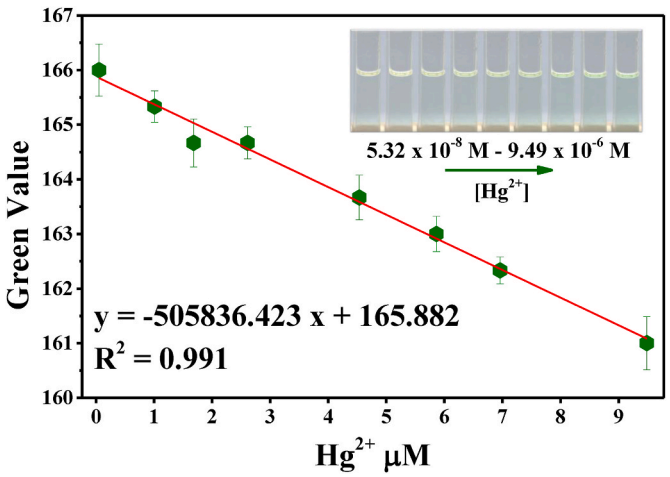

Fig. 6. Smartphone assisted Hg^{2+} ion detection with **NIR-12** in EtOH/H_2O (3/1, v/v, pH 7.4 HEPES). Inset: colorimetric changes with addition of Hg^{2+}.

probe **NIR-12** titrated with Hg^{2+} ions along with the resulting linear range. In summary, Hg^{2+} ions can be effectively detected using the probe **NIR-12** with a smartphone camera, without the need for instrumentation.

3.10. Comparison of analytical performance with similar sensor systems

Recent papers about chemosensors for Hg^{2+} ion detection have yielded a variety of performance metrics. Du et al. reported a rhodamine based probe having a LOD of 0.332 nM towards Hg^{2+} ions and applicability in living cells. Hong et al. developed a rhodamine based probe with a LOD of 0.304 μM and suitability for determination of Hg^{2+} ions in real water samples. Liu and Qian published a study with a probe having a LOD of 2.72 μM for Hg^{2+} ions. Zhang et al. synthesized a rhodamine based probe demonstrating a LOD of 0.38 μM and utility for cell imaging. Biswal et al. reported two rhodamine-pyrrole based probes exhibiting LOD of 0.6 nM and applicability in cell imaging for Hg^{2+} ions. Drawing on the insights from these documents summarized above, this particular study was focused on a chemosensor that addressing existing limitations by providing enhanced functionality in aspects of response time, selectivity, wide linear range and applicability for real water examples. The comparison of these probes with probe **NIR-12** is outlined in Table 2 below. As illustrated in the table, the probe developed in this study above stands out among the existing studies in the literature with its long absorption/emission wavelength, wide working range, excellent selectivity, low LOD values, very fast response time and practical applications in real water samples.

4. Conclusion

In summary, we present an innovative near-infrared (NIR), "ratiometric," and "turn-on" fluorescence probe, **NIR-12**, which is built on a chromenylium cyanine framework and functionalized with 2-amino-5-bromothiazole. The probe is capable of rapid, selective, sensitive, and on-site recognition of Hg^{2+} ions in real samples. Structural characterization and sensor studies using NMR, FT-IR, HR-MS, UV-Vis, and fluorescence spectroscopy revealed that the non-fluorescent probe **NIR-12** selectively interacts with Hg^{2+} ions. This interaction induces a spirolactam ring opening, leading to intense absorption and emission signals in NIR area, and an observable color shift distinguishable with human eye. The developed probe **NIR-12** exhibits superior performance: i) **NIR-12** has ultra-fast response (10 s) and excellent selectivity towards Hg^{2+} ions in EtOH/H_2O (3/1, v/v, pH 7.4) medium, ii) **NIR-12** also has significant linear ranges (1.68-9.81 μM for UV-Vis and 0.85-42.98 μM for fluorescence methods) and LODs (0.057 μM (11.40 ppb) for UV-Vis, 0.277 μM (55.53 ppb) for fluorescence), iii) **NIR-12** is proven to be capable for the measurement Hg^{2+} ions in real drinking water samples, exhibiting high recovery values (95.13% - 106.62%), and iv) **NIR-12** makes Hg^{2+} detection practical and on-site, thanks to its smartphone-assisted measurements. The collective results indicate that the developed spectrophotometric and colorimetric methods based on the **NIR-12** probe provide a simple and practical means of analyzing toxic Hg^{2+} ions, which pose a significant threat to human health.

It is believed that the chromenylium cyanine-based probe developed for Hg^{2+} analysis in this study will serve as a model for the design of new

Table 2
Comparison of analytical performance with similar sensor systems.

Sensor	Medium	Absorption/Emission Wavelength (nm)	Selectivity	Linear Range UV-Vis/Fluorescence	LOD for UV-Vis/Fluorescence	Response Time	Application	Reference
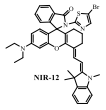	**EtOH/H_2O (3/1, v/v, pH = 7.4)**	**717/740**	**Only Hg^{2+}**	1.68-9.81 μM/0.85-42.98 μM	0.057 μM/0.277 μM	**10 s**	**Smartphone, Drinking Water Samples**	**This Study**
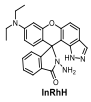	CH_3CN/H_2O (1/4,v/v pH = 6.0)	510/590	Only Hg^{2+}	0.5 μM - 3.0 μM	0.332 nM	40 min	Cell imaging	[39]
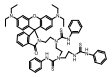	CH_3CN/HEPES (9/1, v/v, pH = 7.21)	565/583	Only Hg^{2+}	25 - 200 μM	0.304 μM	30 min	Water samples	[40]
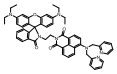	EtOH/PBS (1/1, v/v, pH = 7.4)	516/578	Hg^{2+} and Fe^{3+}	0 - 80 μM	2.72 μM	2 s	Nd.	[41]
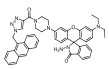	CH_3CN/H_2O (1/1, v/v)	554/608	Hg^{2+} and Cu^{2+}	0 - 30 μM 15 - 45 μM	0.38 μM/0.81 μM	30 s	Cell imaging	[42]
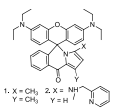	CH_3CN/H_2O (1/1, v/v, PBS buffer, pH = 7.2)	558/580	Hg^{2+}, Fe^{2+} and Pb^{2+}	0.2 - 100 μM	Probe 1: 0.6 nM Probe 2: 2.7 nM	15 min	Nd.	[43]

*Nd. = No data.

probes for the analysis of other toxic chemicals.

CRediT authorship contribution statement

Utku Ertugral: Writing – original draft, Validation, Methodology, Investigation, Formal analysis, Data curation. **Hulya Aribuga:** Writing – original draft, Validation, Methodology, Investigation, Formal analysis, Data curation. **Ozgur Yavuz:** Validation, Methodology, Investigation, Formal analysis, Data curation. **Emre Ozdemir:** Visualization, Methodology, Investigation, Formal analysis, Data curation. **Yusuf Alcay:** Validation, Methodology, Investigation, Formal analysis, Data curation. **Nebahat Ejder:** Writing – original draft, Validation, Methodology, Investigation, Formal analysis, Data curation. **Ismail Yilmaz:** Writing – review & editing, Supervision, Project administration, Investigation, Funding acquisition, Conceptualization.

Declaration of competing interest

The authors declare that they have no known competing financial interests or personal relationships that could have appeared to influence the work reported in this paper.

Acknowledgments

This work was supported by the Council of Higher Education (YOK)-Istanbul Technical University (ITU) Research Fund YAP (Project No.: TGA-2023-43934). The authors thank to YOK and ITU for their supports.

Appendix A. Supplementary data

Supplementary data to this article can be found online at https://doi.org/10.1016/j.dyepig.2026.113902.

Data availability

Data will be made available on request.

References

[1] Aribuga H, Ertugral U, Alcay Y, Yavuz O, Yildirim MS, Ozdemir E, Kaya K, Sert ABO, Kok FN, Tuzun NŞ, Yilmaz I. A new Fe3+-selective, sensitive, and dual-channel turn-on probe based on rhodamine carrying thiophenecarboxaldehyde: smartphone application and imaging in living cells. Spectrochim Acta Mol Biomol Spectrosc 2023;287:122060. https://doi.org/10.1016/j.saa.2022.122060.

[2] Kaplan M, Yavuz O, Ozdemir E, Alcay Y, Kaya K, Yilmaz I. Architecture of easy-to-synthesize and superior probe based on aminoquinoline appended naphthoquinone: instant and On-Site Cu2+ ion quantification in real samples and unusual crystal structure and logic gate operations. Inorg Chem 2024;63:2257–67. https://doi.org/10.1021/acs.inorgchem.3c04229.

[3] Yavuz O, Alcay Y, Kaya K, Sezen M, Kirlangic Atasen S, Yildirim MS, Ozkilic Y, Tuzun NŞ, Yilmaz I. Superior sensor for Be2+ ion recognition via the unprecedented octahedral crystal structure of a one-dimensional coordination polymer of crown fused zinc phthalocyanine. Inorg Chem 2019;58:909–23. https://doi.org/10.1021/acs.inorgchem.8b03038.

[4] Alcay Y, Yavuz O, Gelir A, Atasen SK, Karaoglu K, Yucel B, Tuzun NŞ, Yilmaz I. New ferrocenyl naphthoquinone fused crown ether chemosensors: highly selective, kinetically and regio controlled colorimetric, beryllium ion recognition. J Organomet Chem 2018;868:131–43. https://doi.org/10.1016/j.jorganchem.2018.05.004.

[5] Karaoglu K, Kaya K, Yilmaz I. New Chromenylium−cyanine based dual channel chemosensors for copper and hypochlorite sensing. Dyes Pigments 2020;180:108445. https://doi.org/10.1016/j.dyepig.2020.108445.

[6] Kaplan M, Yavuz O, Alcay Y, Yilmaz I. Development of a new aminophenol-extended naphthoquinone-based chemical sensor with superior performance and easy accessibility for on-site and instantaneous determination of Cu2+ ions in selected environmental and food samples. Food Chem 2025;491:145182. https://doi.org/10.1016/j.foodchem.2025.145182.

[7] Ali H, Khan E, Ilahi I. Environmental chemistry and ecotoxicology of hazardous heavy metals: environmental persistence, toxicity, and bioaccumulation. J Chem 2019 2019:6730305. https://doi.org/10.1155/2019/6730305.

[8] Rustagi N, Singh R. Mercury and health care. Indian J Occup Environ Med 2010;14:45. https://doi.org/10.4103/0019-5278.72240.

[9] Tibau AV, Grube BD. Mercury contamination from dental amalgam. J Health Pollut 2019;9:190612. https://doi.org/10.5696/2156-9614-9.22.190612.

[10] Gworek B, Dmuchowski W, Baczewska-Dąbrowska AH. Mercury in the terrestrial environment: a review. Environ Sci Eur 2020;32:128. https://doi.org/10.1186/s12302-020-00401-x.

[11] Wu Y-S, Osman AI, Hosny M, Elgarahy AM, Eltaweil AS, Rooney DW, Chen Z, Rahim NS, Sekar M, Gopinath SCB, Mat Rani NNI, Batumalaie K, Yap P-S. The toxicity of mercury and its chemical compounds: molecular mechanisms and environmental and human health implications: a comprehensive review. ACS Omega 2024;9:5100–26. https://doi.org/10.1021/acsomega.3c07047.

[12] O'Connor LE, Spill MK, Trivedi R, Saha S, Thoerig RC, Foster M, MacFarlane AJ. Mercury exposure and childhood outcomes: an overview of systematic reviews. Environ Res 2025;274:121196. https://doi.org/10.1016/j.envres.2025.121196.

[13] Park J-D, Zheng W. Human exposure and health effects of inorganic and elemental mercury. J Prev Med Publ Health 2012;45:344–52. https://doi.org/10.3961/jpmph.2012.45.6.344.

[14] US EPA O. What EPA is doing to reduce mercury pollution, and exposures to mercury. https://www.epa.gov/mercury/what-epa-doing-reduce-mercury-pollution-and-exposures-mercury. [Accessed 10 November 2025].

[15] Sarkar PK, Polley N, Chakrabarti S, Lemmens P, Pal SK. Nanosurface energy transfer based highly selective and ultrasensitive "Turn on" fluorescence mercury sensor. ACS Sens 2016;1:789–97. https://doi.org/10.1021/acssensors.6b00153.

[16] Fernández ZH, Valcárcel Rojas LA, Álvarez AM, Estevez Álvarez JR, Araújo Dos Santos J, González IP, González MR, Macias NA, Sánchez DL, Torres DH. Application of cold vapor-atomic absorption (CVAAS) spectrophotometry and inductively coupled plasma-atomic emission spectrometry methods for cadmium, mercury and lead analyses of fish samples. Validation of the method of CVAAS. Food Control 2015;48:37–42. https://doi.org/10.1016/j.foodcont.2014.05.056.

[17] Panichev NA, Panicheva SE. Determination of total mercury in fish and sea products by direct thermal decomposition atomic absorption spectrometry. Food Chem 2015;166:432–41. https://doi.org/10.1016/j.foodchem.2014.06.032.

[18] Palanna M, Aralekallu S, Keshavananda Prabhu C, Sajjan VA, Mounesh Sannegowda LK. Nanomolar detection of mercury(II) using electropolymerized phthalocyanine film. Electrochim Acta 2021;367:137519. https://doi.org/10.1016/j.electacta.2020.137519.

[19] Chandrasoma A, Hamid AAA, Bruce AE, Bruce MRM, Tripp CarlP. An infrared spectroscopic based method for mercury(II) detection in aqueous solutions. Anal Chim Acta 2012;728:57–63. https://doi.org/10.1016/j.aca.2012.03.047.

[20] da Silva DLF, da Costa MAP, Silva LOB, dos Santos WNL. Simultaneous determination of mercury and selenium in fish by CVG AFS. Food Chem 2019;273:24–30. https://doi.org/10.1016/j.foodchem.2018.05.020.

[21] Alcay Y, Ozdemir E, Yildirim MS, Ertugral U, Yavuz O, Aribuga H, Ozkilic Y, Şenyurt Tuzun N, Ozdabak Sert AB, Kok FN, Yilmaz I. A methionine biomolecule-modified chromenylium-cyanine fluorescent probe for the analysis of Hg2+ in the environment and living cells. Talanta 2023;259:124471. https://doi.org/10.1016/j.talanta.2023.124471.

[22] Basan V, Alcay Y, Ozdemir E, Gunduz MI, Kura B, Tuzun NŞ, Cil C, Kilic A, Yilmaz I. Architecture of a novel NIR and switch-on fluorescent chemosensor based on mercapto propanehydrazide-functionalized chromenylium-cyanine for the quantification of mercury(II) in environment and living cells. Spectrochim Acta Mol Biomol Spectrosc 2025;329:125589. https://doi.org/10.1016/j.saa.2024.125589.

[23] Mermer Z, Yavuz O, Atasen SK, Alcay Y, Yilmaz I. Architecture of multi-channel and easy-to-make sensors for selective and sensitive Hg2+ ion recognition through Hg−C and hg-n bonds of naphthoquinone-aniline/pyrene union. J Hazard Mater 2021;410:124597. https://doi.org/10.1016/j.jhazmat.2020.124597.

[24] Yildirim MS, Alcay Y, Ozdemir E, Ertugral U, Yavuz O, Aribuga H, Kaya K, Ozkilic Y, Tuzun NŞ, Sert ABO, Yilmaz I. Molecular architecture of a novel indoline-fused chromenylium-cyanine probe carrying methionine biomolecule for ultrasensitive analyzing Hg2+ ion in real samples. J Environ Chem Eng 2024;12:114388. https://doi.org/10.1016/j.jece.2024.114388.

[25] Ejder N, Karaoglu K, Levent Z, Alcay Y, Ozdemir E, Yavuz O, Kaya K, Kopar M, Tuzun NŞ, Yilmaz I. Colorimetric and fluorimetric sensing of trace amount of Hg2+ in real samples by a new rhodamine B-based Schiff base probe: smartphone, living cell applications and DFT calculation. J Mol Struct 2025;1321:139687. https://doi.org/10.1016/j.molstruc.2024.139687.

[26] Niu H, Ye T, Yao L, Lin Y, Chen K, Zeng Y, Li L, Guo L, Wang J. A novel red-to-near-infrared AIE fluorescent probe for detection of Hg2+ with large stokes shift in plant and living cells. J Hazard Mater 2024;475:134914. https://doi.org/10.1016/j.jhazmat.2024.134914.

[27] Yang Y-K, Yook K-J, Tae J. A rhodamine-based fluorescent and colorimetric chemodosimeter for the rapid detection of Hg2+ ions in aqueous media. J Am Chem Soc 2005;127:16760–1. https://doi.org/10.1021/ja054855t.

[28] Bai C-B, Xu P, Zhang J, Qiao R, Chen M-Y, Mei M-Y, Wei B, Wang C, Zhang L, Chen S-S. Long-wavelength fluorescent chemosensors for Hg2+ based on pyrene. ACS Omega 2019;4:14621–5. https://doi.org/10.1021/acsomega.9b02078.

[29] Kırpık H, Kose M, Elmes RBP, Karabork M. BODIPY- imine based fluorescence "turn on" chemosensor for selective sensing of Hg2+. J Photochem Photobiol Chem 2024;451:115541. https://doi.org/10.1016/j.jphotochem.2024.115541.

[30] Wang J, Qian X, Cui J. Detecting Hg2+ ions with an ICT fluorescent sensor molecule: remarkable emission spectra shift and unique selectivity. J Org Chem 2006;71:4308–11. https://doi.org/10.1021/jo052642g.

[31] Muthusamy S, Zhao L, Rajalakshmi K, Zhu D, Wang S, Mack J, Lee K-B, Zhang L, Zhu W. Quantitative Hg2+ detection via forming three coordination complexes using a lysosome targeting quinoline - fisher aldehyde fluorophore. Talanta 2022;236:122884. https://doi.org/10.1016/j.talanta.2021.122884.

[32] Li G, Guan Y, Ye F, Liu SH, Yin J. Cyanine-based fluorescent indicator for mercury ion and bioimaging application in living cells. Spectrochim Acta Mol Biomol Spectrosc 2020;239:118465. https://doi.org/10.1016/j.saa.2020.118465.
[33] Qi Y-L, Li Y-Z, Tan M-J, Yuan F-F, Murthy N, Duan Y-T, Zhu H-L, Yang S-Y. Recent advances in organic near-infrared ratiometric small-molecule fluorescent probes. Coord Chem Rev 2023;486:215130. https://doi.org/10.1016/j.ccr.2023.215130.
[34] Li B, Wang J, Peng Y, Liu C, Ming Y, Yang B, He D, Lai W, Guo L, Zhao M, Chen X. BODIPY-doped nanocarrier engineering (BONE) improves bone marrow mRNA delivery by NIR-II bioimaging guided screening. J Am Chem Soc 2026;148: 4966–75. https://doi.org/10.1021/jacs.5c14271.
[35] Park H, Oh E-T, Park J, Subedi S, Park HJ, Lee K-H. Real-time detection of methylmercury and Hg(II) using a reversible ratiometric fluorescent probe in cellular and aqueous environments. Anal Chem 2025;97:5982–91. https://doi.org/10.1021/acs.analchem.4c05362.
[36] Park H, Subedi S, Oh E-T, Joo Park H, Lee K-H. Fluorescent turn-on detection of inorganic mercury and methylmercury in aqueous solution with PC micelles and live cells using fluorescent chemosensors based on Trp amino acid and cycloalkylamine-7-sulfonyl-2,1,3-benzoxadiazole. Microchem J 2024;200:110375. https://doi.org/10.1016/j.microc.2024.110375.
[37] Ozdemir E, Alcay Y, Yavuz O, Yildirim MS, Aribuga H, Ertugral U, Kaya K, Yilmaz I. Colorimetric and near-infrared spectrophotometric monitoring of bisulfite using glyoxal modified chromenylium-cyanine chemosensor: smartphone and paper strip applications for on-site food and beverages control. Talanta 2023;261:124660. https://doi.org/10.1016/j.talanta.2023.124660.
[38] Alçay Y. A green and practical approach to chromenylium–cyanine dye synthesis using triethylammonium hydrogen sulfate as an alternative to acetic anhydride. J Anatol Environ Anim Sci 2025;10:978–85. https://doi.org/10.35229/jaes.1737673.
[39] Du B, Li Q, Huang K, Wang Q, Liang L. Mercury ion-selective fluorescent probe based on indazole fused rhodamine and cell imaging application. J Photochem Photobiol Chem 2023;436:114419. https://doi.org/10.1016/j.jphotochem.2022.114419.
[40] Hong M, Lu S, Lv F, Xu D. A novel facilely prepared rhodamine-based Hg2+ fluorescent probe with three thiourea receptors. Dyes Pigments 2016;127:94–9. https://doi.org/10.1016/j.dyepig.2015.12.023.
[41] Liu J, Qian Y. A novel naphthalimide-rhodamine dye: intramolecular fluorescence resonance energy transfer and ratiometric chemodosimeter for Hg2+ and Fe3+. Dyes Pigments 2017;136:782–90. https://doi.org/10.1016/j.dyepig.2016.09.041.
[42] Zhang Q, Ding H, Xu X, Wang H, Liu G, Pu S. Rational design of a FRET-based ratiometric fluorescent probe with large pseudo-stokes shift for detecting Hg2+ in living cells based on rhodamine and anthracene fluorophores. Spectrochim Acta Mol Biomol Spectrosc 2022;276:121242. https://doi.org/10.1016/j.saa.2022.121242.
[43] Biswal B, Mallick D, Bag B. Signaling preferences of substituted pyrrole coupled six-membered rhodamine spirocyclic probes for Hg2+ ion detection. Org Biomol Chem 2016;14:2241–8. https://doi.org/10.1039/C5OB02606G.
[44] Yuan L, Lin W, Yang Y, Chen H. A unique class of near-infrared functional fluorescent dyes with carboxylic-acid-modulated fluorescence ON/OFF switching: rational design, synthesis, optical properties, theoretical calculations, and applications for fluorescence imaging in living animals. J Am Chem Soc 2012;134: 1200–11. https://doi.org/10.1021/ja209292b.
[45] Rasheed T, Nabeel F, Bilal M, Zhao Y, Adeel M, Iqbal HMN, Rasheed T, Nabeel F, Bilal M, Zhao Y, Adeel M, Iqbal HMN. Aqueous monitoring of toxic mercury through a rhodamine-based fluorescent sensor. Math Biosci Eng 2019;16:1861–73. https://doi.org/10.3934/mbe.2019090.
[46] Sun Y, Zuo S, Li Z, Li P, Hu J. Thiazolo[5,4-*d*]thiazole conjugated microporous polymers for efficient removal of Hg(II) from wastewater. J Colloid Interface Sci 2026;702:138839. https://doi.org/10.1016/j.jcis.2025.138839.
[47] Nath A, Thomas GM, Hans S, Vennapusa SR, Mandal S. Crystal packing-driven selective Hg(II) ion sensing using Thiazolothiazole-Based water-stable zinc metal–organic framework. Inorg Chem 2022;61:2227–33. https://doi.org/10.1021/acs.inorgchem.1c03534.
[48] Subedi S, Neupane LN, Mehta PK, Lee K-H. Ratiometric fluorescent detection of Hg (II) by amino-acid based fluorescent chemodosimeter using irreversible reaction of phenylboronic acid with mercury species. Dyes Pigments 2021;191:109374. https://doi.org/10.1016/j.dyepig.2021.109374.